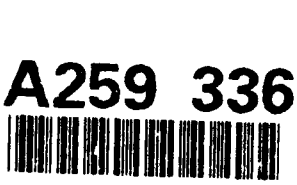

(12)

MASSACHUSETTS INSTITUTE OF TECHNOLOGY
ARTIFICIAL INTELLIGENCE LABORATORY

A.I. Memo No. 1303 December 1991

Automatic Design of a Maglev Controller in State Space

Feng Zhao Richard Thornton

Abstract

We describe the automatic synthesis of a global nonlinear controller for stabilizing a magnetic levitation system—a simplified model for the German Transrapid system. A systematic state-space design method for determining the global switching points of the controller is presented. The synthesized control system can stabilize the maglev vehicle with large initial displacements from an equilibrium, and possesses a much larger operating region than the classical linear feedback design for the same system.

The controller is automatically synthesized by a suite of computational tools that visualize and model the state-space geometry and topology of a given system, use a novel technique of "flow pipes" to plan global reference trajectories in state space, and navigate the system along the planned trajectories. This work demonstrates that the difficult control synthesis task can be automated, using programs that actively exploit knowledge of nonlinear dynamics and state space and combine powerful numerical and symbolic computations with spatial-reasoning techniques.

Keywords. Magnetic levitation; control system synthesis; state-space methods; artificial intelligence; numeric/symbolic processing; computer-aided design.

This paper describes research done at the Artificial Intelligence Laboratory of the Massachusetts Institute of Technology. Support for the Laboratory's artificial intelligence research is provided in part by the Advanced Research Projects Agency of the Department of Defense under Office of Naval Research contract N00014-89-J-3202, and in part by the National Science Foundation grant MIP-9001651.

REPORT DOCUMENTATION PAGE

Form Approved
OMB No 0704-0188

1. AGENCY USE ONLY (Leave blank)	2. REPORT DATE	3. REPORT TYPE AND DATES COVERED
	December 1991	memorandum

4. TITLE AND SUBTITLE

Automation Desing of a Maglev Controller in State Space

5. FUNDING NUMBERS

N00014-89-J-3202
MIP-9001651

6. AUTHOR(S)

Feng Zhao and Richard Thornton

7. PERFORMING ORGANIZATION NAME(S) AND ADDRESS(ES)

Artificial Intelligence Laboratory
545 Technology Square
Cambridge, Massachusetts 02139

8. PERFORMING ORGANIZATION REPORT NUMBER

AIM 1303

9. SPONSORING/MONITORING AGENCY NAME(S) AND ADDRESS(ES)

Office of Naval Research
Information Systems
Arlington, Virginia 22217

10. SPONSORING/MONITORING AGENCY REPORT NUMBER

11. SUPPLEMENTARY NOTES

None

12a. DISTRIBUTION/AVAILABILITY STATEMENT

Distribution of this document is unlimited

12b. DISTRIBUTION CODE

13. ABSTRACT *(Maximum 200 words)*

We describe the automatic synthesis of a global nonlinear controller for stabilizing a magnetic levitation system—a simplified model for the German Transrapid system. A systematic state-space design method for determining the global switching points of the controller is presented. The synthesized control system can stabilize the maglev vehicle with large initial displacements from an equilibrium, and possesses a much larger operating region than the classical linear feedback design for the same system.

The controller is automatically synthesized by a suite of computational tools that visualize and model the state-space geometry and topology of a

(continued on back)

14. SUBJECT TERMS (key words)

magnetic levitation
state-space methods
computer-aided design
control system synthesis
artificial intelligence
numeric/symbolic processing

15. NUMBER OF PAGES 18

16. PRICE CODE

17. SECURITY CLASSIFICATION OF REPORT	18. SECURITY CLASSIFICATION OF THIS PAGE	19. SECURITY CLASSIFICATION OF ABSTRACT	20. LIMITATION OF ABSTRACT
UNCLASSIFIED	UNCLASSIFIED	UNCLASSIFIED	UNCLASSIFIED

Block 13 continued:

given system, use a novel technique of "flow pipes" to plan global reference trajectories in state space, and navigate the system along the planned trajectories. This work demonstrates that the difficult control synthesis task can be automated, using programs that actively exploit knowledge of nonlinear dynamics and state space and combine powerful numerical and symbolic computations with spatial-reasoning techniques.

Automatic Design of a Maglev Controller in State Space

Feng Zhao Richard Thornton
Department of Electrical Engineering and Computer Science
Massachusetts Institute of Technology
Cambridge, MA 02139

December 1991

Abstract

We describe the automatic synthesis of a global nonlinear controller for stabilizing a magnetic levitation system—a simplified model for the German Transrapid system. A systematic state-space design method for determining the global switching points of the controller is presented. The synthesized control system can stabilize the maglev vehicle with large initial displacements from an equilibrium, and possesses a much larger operating region than the classical linear feedback design for the same system.

The controller is automatically synthesized by a suite of computational tools that visualize and model the state-space geometry and topology of a given system, use a novel technique of "flow pipes" to plan global reference trajectories in state space, and navigate the system along the planned trajectories. This work demonstrates that the difficult control synthesis task can be automated, using programs that actively exploit knowledge of nonlinear dynamics and state space and combine powerful numerical and symbolic computations with spatial-reasoning techniques.

Keywords. Magnetic levitation; control system synthesis; state-space methods; artificial intelligence; numeric/symbolic processing; computer-aided design.

1 Introduction

Magnetically levitated trains provide a high speed, very low friction alternative to conventional trains with steel wheels on steel rails. Several experimental maglev systems in Germany and Japan have demonstrated that this mode of transportation can profitably compete with air travel. More importantly, maglev transportation can ease traffic congestion and save energy [2, 3, 5].

The maglev transportation uses magnetic levitation and electromagnetic propulsion to provide contactless vehicle movement. There are two basic types of magnetic levitation: electromagnetic suspension (EMS) and electrodynamic suspension (EDS). In EMS, the guideway attracts the electromagnets of the vehicle that wraps around the guideway. The attracting force suspends the vehicle about one centimeter above the guideway. In contrast, the EDS system uses repulsive force, induced by the magnets on the vehicle, to lift the vehicle.

2 The Maglev Model

An attractive system such as the EMS system is inherently unstable. We consider the control design for stabilizing an EMS-mode train traveling on a guideway—a simplified model for the German Transrapid experimental system. The Transrapid system is schematically shown in Figure 1. It uses attractive magnetic forces to counterbalance gravitational forces.

The state equations for the magnetically levitated vehicle and the guideway are described by

$$\begin{cases} \dfrac{dx}{dt} = \dfrac{z(V_i - Rx)}{L_0 z_0} + \dfrac{xy}{z} \\ \dfrac{dy}{dt} = g - \dfrac{L_0 z_0 x^2}{2mz^2} \\ \dfrac{dz}{dt} = y \end{cases} \tag{1}$$

where the state variables x, y, and z represent coil current, vertical velocity of the vehicle, and vertical gap between the guideway and the vehicle, respectively. The control parameter is the coil input voltage V_i. The other parameters are the mass of the vehicle m, the coil resistance R, the coil inductance L_0 and the vertical gap z_0 at the equilibrium, and the gravitational acceleration g. Details of the derivation of the model are discussed in [4].

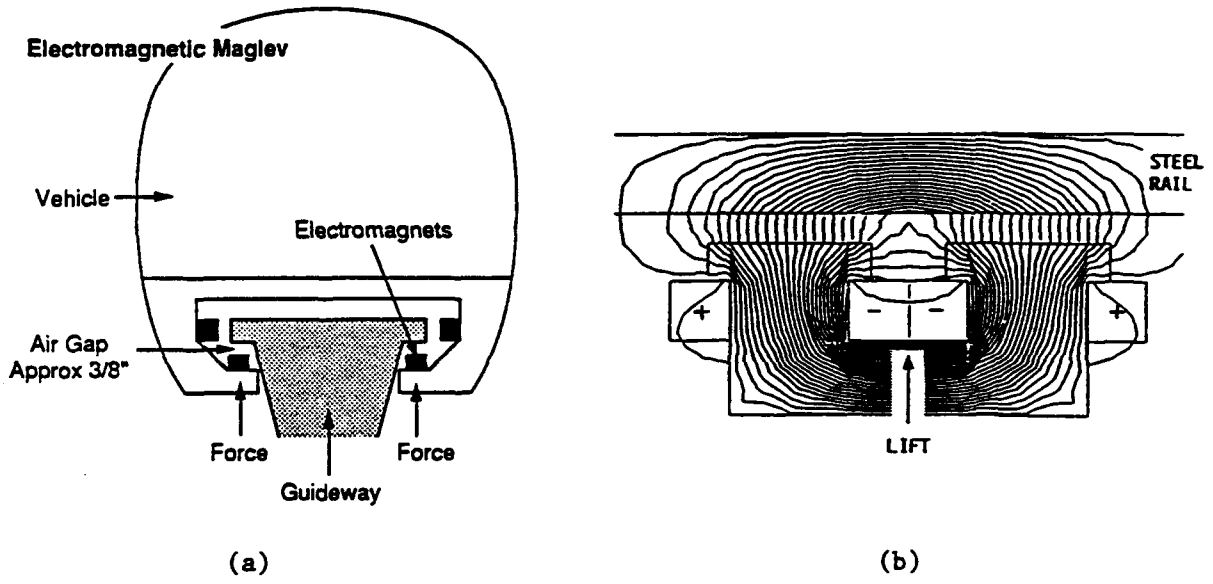

Figure 1: EMS maglev system for high-speed ground transportation, representing a simplified drawing of the German Transrapid design. (a) Electromagnetic suspension; (b) Detail of a suspension magnet, superimposed on the field distribution.

The system has one equilibrium state at which the magnetic force exactly counterbalances the force due to gravity and the vehicle has no vertical velocity and acceleration. However, the equilibrium is a saddle node which is not stable. The control objective, therefore, is to stabilize the vehicle traveling down the guideway and maintain a constant distance between the vehicle and the guideway despite any roughness in the guideway. The available control input is the coil input voltage V_i, as in the model (1). We further assume that V_i is produced by a buck converter capable of delivering any voltage from 0 to 300 volts.

A linear control design for the maglev system described in [4] uses the pole-placement method. The system is first linearized around the equilibrium. The linearized system has unstable poles, i.e., the poles in the right-half of s-plane. A linear feedback is introduced to move the poles to the desired locations in the left-half of the s-plane. Such a control design can bring the system back to the equilibrium with an initial displacement of 0.2mm from the equilibrium. The linear controller saturates at the beginning for larger initial displacements. This is because the linearized model no longer approximates the original system well in regions far away from the equilibrium. A nonlinear control law such as a bang-bang control that respects the nonlinearities of the system is, therefore, necessary to proceed the linear feedback control. However, the real challenge for the nonlinear design is to determine the global control switching points.

3 State-Space Control Trajectory Design

We demonstrate a nonlinear control design—a switching-mode control—for the maglev system with large initial displacements from the equilibrium. We also present an automatic method for designing such a controller. The nonlinear controller brings the system to the vicinity of the equilibrium and then switches to the linear controller.

For the purpose of demonstration, we assume that the vehicle is displaced from the equilibrium in the direction further away from the guideway. We will concentrate on the global design of the control reference trajectories and assume that a linear feedback design is available as soon as the system enters the capture region of the linear controller.

3.1 Modeling state-space geometry and topology

The global control law is designed by exploiting the nonlinear dynamics in state space. We have developed a suite of computational tools for the design and analysis of nonlinear control systems. The two main programs, MAPS and Phase Space Navigator, work together to visualize and model the state-space geometry and topology of a given system, plan global reference trajectories in state space, and navigate the system along the planned trajectories. MAPS computationally explores the state space of a dynamical system and characterizes the state space with stability regions and trajectory flow pipes that bundle together trajectories with the same qualitative features [6]. Phase Space Navigator uses the state-space characterizations for different control parameter values to synthesize a composite reference trajectory, consisting of path segments connected at intermediate points where control parameters change [7].

We ran MAPS on the maglev model. The state variables x, y, and z in the model are scaled by 1, 10^3, and 2×10^4, respectively. The parameters of model are assumed to be: $L_0 = 0.1h$, $z_0 = 0.01m$, $R = 1\Omega$, $m = 10000kg$ and $g = 9.8m/sec^2$, typical of a large vehicle lift magnet. Assume at the equilibrium, the power supply delivers 140 volts, i.e., $V_i = 140$. MAPS explores in a region of the state space bounded by the box $\{(x,y,z)|x \in [0,400], y \in [-300,350], z \in [0,600]\}$ and finds the following equilibrium point:

```
saddle:       #(140. 0. 200.)
eigenvalues:  -17.004+22.963i
              -17.004-22.963i
              24.007
eigenvectors: #(.23604 .97174 0)
              #(.51331 -.55588 .65384)
              #(.30157 .73255 .61027)
```

With the information about the stable eigenvectors of the saddle, MAPS computationally determines the stable manifold (often called separatrix) of the saddle. MAPS uses a set of trajectories evenly populated on the stable manifold to approximate the manifold. The set of trajectories are obtained by backward integrations starting at initial points in the plane spanned by the stable eigenvectors within a small neighborhood of the saddle. The stable

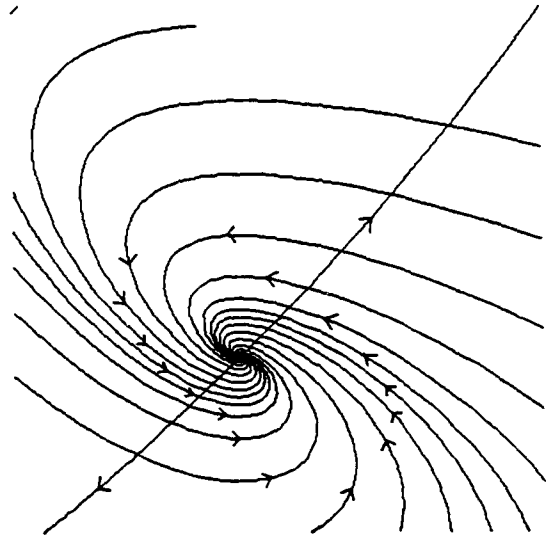

Figure 2: Stable and unstable manifolds of the saddle for $V_i = 140$ (yz-projection).

manifold is geometrically modeled by a tessellation on these trajectory points with a triangulation method.

Figure 2 shows the trajectories on the stable manifold and along the unstable eigenvectors of the saddle in the yz-projection of the state space. The stable manifold of the saddle separates the state space into two halves: trajectories in the upper-half approach $z \to \infty$ along one of the unstable eigenvectors, corresponding to the case in which the vehicle falls off the rail; and trajectories in the lower-half approach $z = 0$ plane along the other unstable eigenvector, corresponding to the case in which the train collides with the rail.

3.2 Synthesizing a global stabilization law

For an initial displacement above or below the equilibrium, the uncontrolled system will follow either a trajectory traveling upwards with increasing z and leaving the bounding box or a trajectory traveling downwards and hitting the $z = 0$ plane. To stabilize the system at the equilibrium, it is necessary to synthesize a new vector field on both sides of the stable manifold so that

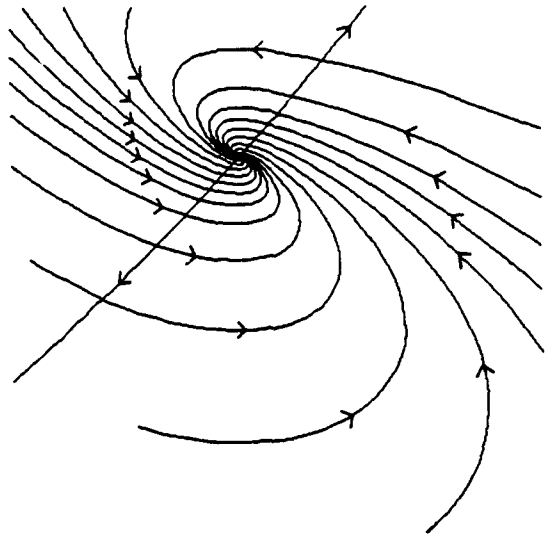

Figure 3: Stable and unstable manifolds of the saddle for $V_i = 300$ (yz-projection).

trajectories travel towards the stable manifold of the saddle. We consider only the top-half here.

Phase Space Navigator first explores the state space of the model for different values of V_i and discovers that the larger the V_i is, the further away the stable manifold is from the $z = 0$ plane. For $V_i = v > 140$, the region sandwiched by the stable manifold of $V_i = 140$ and that of $V_i = v$ has the desired property—the vector field of $V_i = v$ in this region is pointed towards the stable manifold of $V_i = 140$. When $v = 300$, the region is maximized.

Similarly, Phase Space Navigator finds that the model with $V_i = 300$ has a saddle node at $(300., 0., 428.57)$. The stable manifold of the saddle has a similar structure as that of $V_i = 140$ case, but with larger z coordinate. The yz-projection of the stable manifold and unstable trajectories for $V_i = 300$ is shown in Figure 3.

Figure 4 shows the yz-projection of the sandwiched region discussed above. The region is bounded by three pieces of triangulated surfaces, the top boundary shown in Figure 5(a), the side one in Figure 5(b), and the bottom one in Figure 5(c), respectively. The top boundary represents the stable manifold of the saddle for $V_i = 300$ and the bottom one for $V_i = 140$.

The trajectories of $V_i = 300$ flow into the region from the side boundary in Figure 5(b) and leave the region at the bottom boundary in Figure 5(c). There is no flow across the top boundary in Figure 5(a).

The Phase Space Navigator determines that the above region consists of two collections of trajectories: the bundle with $V_i = 300$ that flow into the region on the side boundary and pierce through the bottom one, and the bundle with $V_i = 140$ on the bottom boundary that approach the desired equilibrium asymptotically. Each bundle of the trajectories is called a flow pipe that groups together a collection of trajectories exhibiting the same qualitative behavior. (For more details about the flow pipes, see Reference [7].) With the flow pipe characterization of the state-space trajectory flows, the Phase Space Navigator searches for control trajectories in this set of flow pipes and finds a sequence of flow pipes that lead to the desired goal: the composite of the trajectory bundles with $V_i = 300$ and $V_i = 140$, glued together at the stable manifold of $V_i = 140$ represented by the bottom boundary. As a result, all the trajectories of $V_i = 300$ within the region can be brought to the equilibrium by switching to $V_i = 140$ as soon as the trajectories hit the bottom boundary.

Since the bottom boundary is an approximation to the true stable manifold, the trajectories of $V_i = 140$ on the boundary can only get close to the desired equilibrium. The closeness depends on the quality of the manifold approximation. As the trajectories enter a small neighborhood of the equilibrium, we use a linear feedback controller, such as the one discussed in [4], to stabilize the system at the equilibrium. Figure 6 and 7 show the synthesized control reference trajectories originating at different initial displacements from the equilibrium: 1mm, 4mm, 4.5mm, and 5mm. The controller is able to recover from the first three initial points that are within the region. The last point is outside the region and thus uncontrollable.

3.3 Evaluating the control design

The synthesized global control law is a switching-mode one that changes parameters at the switching surface—the stable manifold of $V_i = 140$. It is able to bring trajectories originating from any states within the controllable region to a local neighborhood of the saddle.

The responses of the controller with respect to the different initial displacements are shown in Figures 8. For all the controllable initial displace-

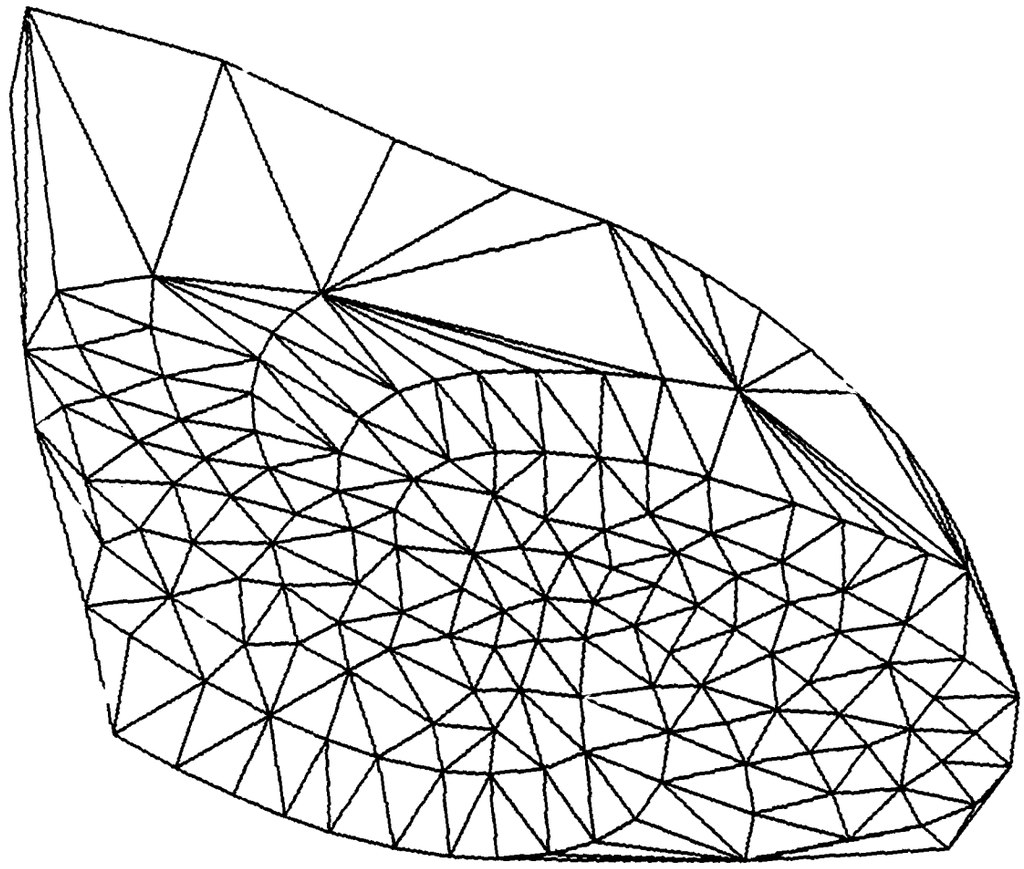

Figure 4: The controllable region in yz-projection.

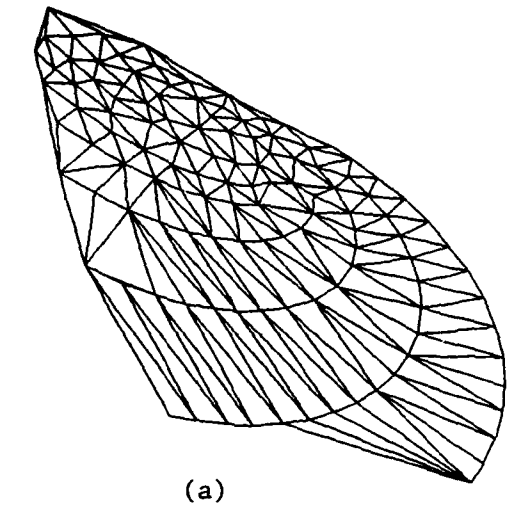

(a)

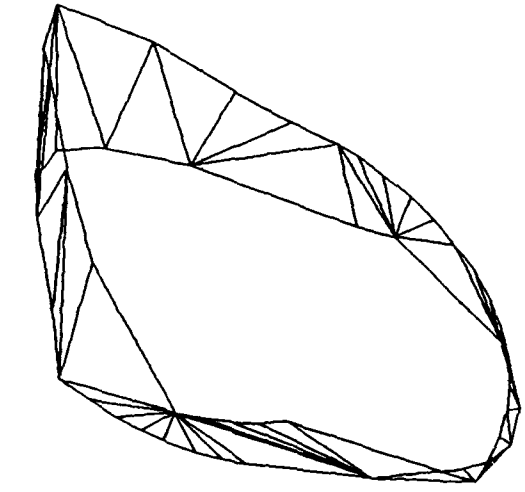

(b)

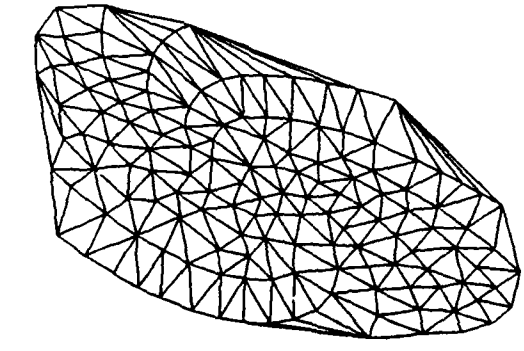

(c)

Figure 5: The boundaries of the controllable region in yz-projection: (a) top boundary; (b) side boundary; (c) bottom boundary.

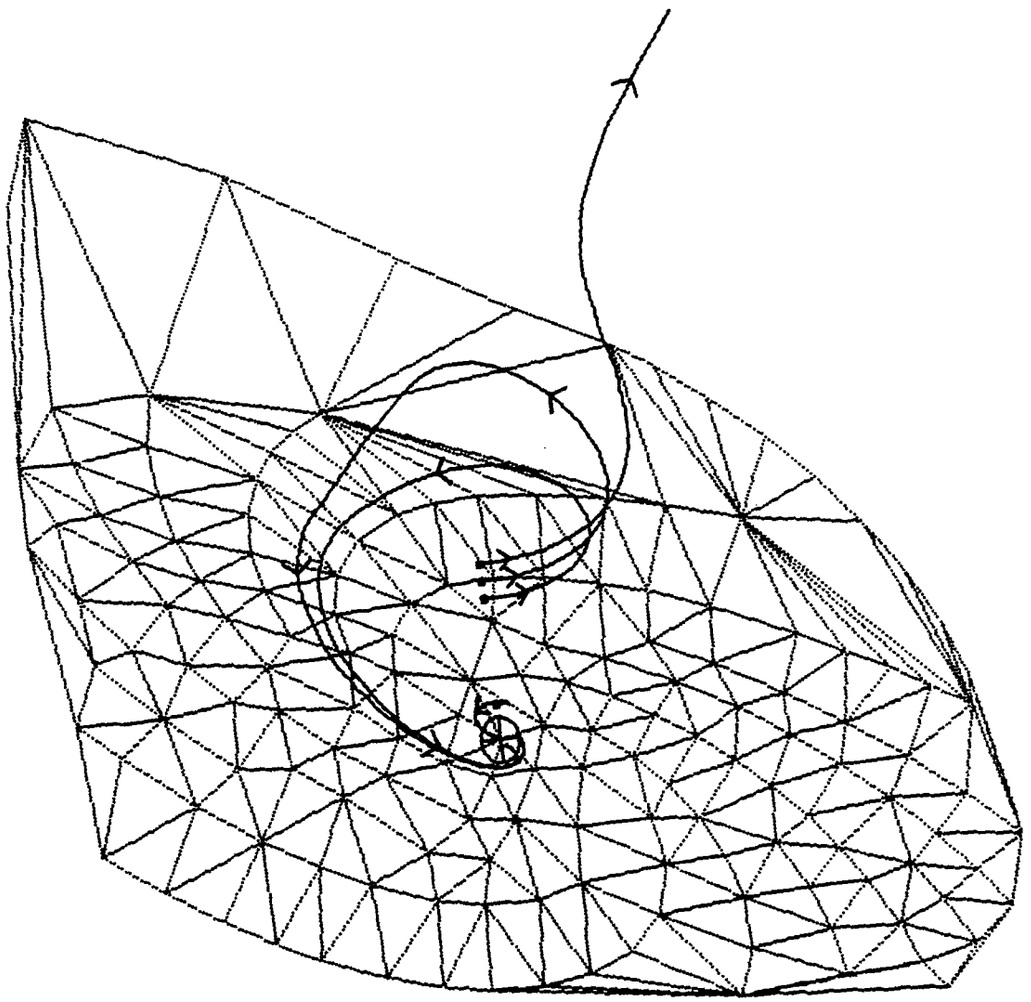

Figure 6: The synthesized control reference trajectories originating from four different initial states, together with the controllable region in yz-projection.

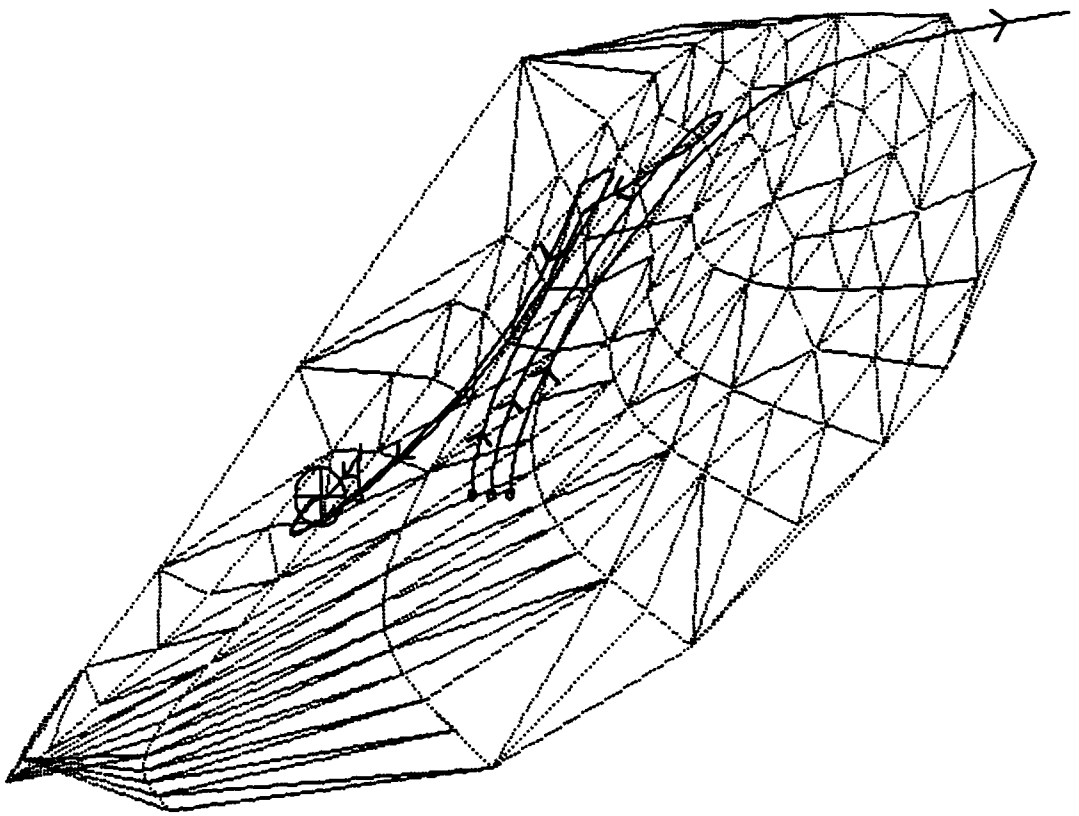

Figure 7: The synthesized control reference trajectories originating from four different initial states, together with the controllable region in zx-projection.

ments, the controller is able to bring the system as close to the equilibrium as within less than 0.2mm in displacement—a distance well captured by the linear feedback controller.

By exploring the state-space geometries of the maglev system, our programs are able to automatically determine the switching points for the global controller. The global controller has significantly enlarged the operating region of the linear feedback controller. With the geometric representation of the controllable region in state space, the programs precisely determined that the maximum recoverable displacement is 4.55mm. Our simulation geometrically explained the observation in [4] that the vehicle would fall off the rails with a displacement of 5mm or larger.

Many issues remain to be addressed in order to make our control design practical. Future work includes the optimization of the design with respect to response time and the study of the effect of uncertainties in the model and noises in the environment on the design.

4 Conclusion

We have designed a high-quality global nonlinear controller for stabilizing an EMS-mode maglev vehicle traveling above guideway. The synthesized control reference trajectory consists of a sequence of trajectory segments, connected at intermediate points where control voltage switches. At runtime, the controller will cause the system to track the reference trajectory and reactively corrects local deviation from the desired trajectory. We have illustrated a systematic method for designing the global switching points of the nonlinear controller. The simulation showed that our design has a much larger maximum recoverable displacement than the classical linear feedback design. This work demonstrates that the difficult control synthesis task can be automated, using programs that actively exploit knowledge of nonlinear dynamics and state space and combine powerful numerical and symbolic computations with spatial-reasoning techniques.

5 Acknowledgment

The authors would like to thank Hal Abelson for comments on the draft of this paper, and George Verghese and Jeff Lang for discussions. The first

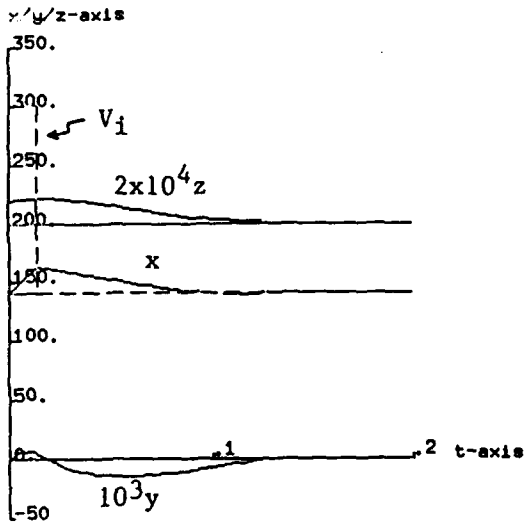

(a) dz=1mm

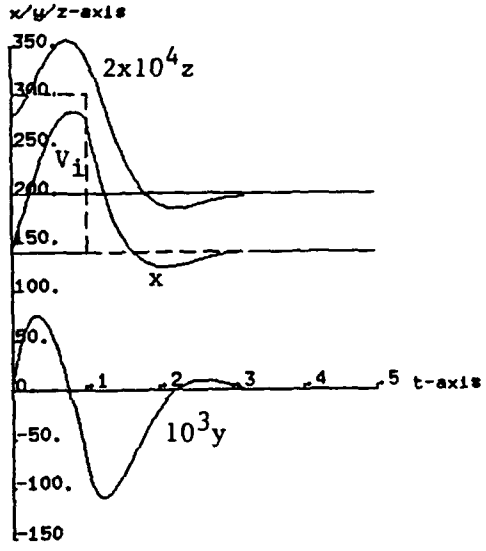

(b) dz=4mm

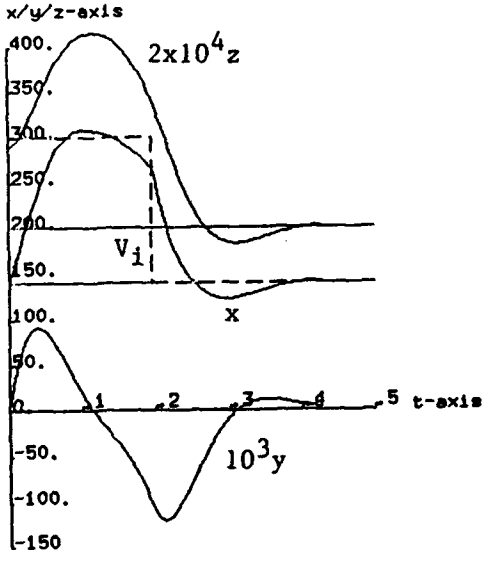

(c) dz=4.5mm

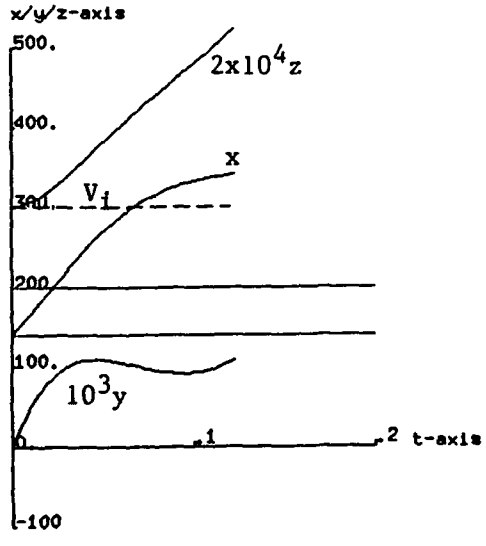

(d) dz=5mm

Figure 8: Simulation of the nonlinear control design with different initial displacements.

author is grateful to Hal Abelson and Gerry Sussman for support and encouragement. Figures 1(a) and (b) are taken from [3] and [2], respectively.

This paper describes research done at the Artificial Intelligence Laboratory of the Massachusetts Institute of Technology, supported in part by the Advanced Research Projects Agency of the Department of Defense under Office of Naval Research contract *N00014-89-J-3202*, and in part by the National Science Foundation grant MIP-9001651.

References

[1] H. Abelson, M. Eisenberg, M. Halfant, J. Katzenelson, E. Sacks, G.J. Sussman, J. Wisdom, and K. Yip, "Intelligence in Scientific Computing." *CACM*, 32(5), May 1989.

[2] T. R. Eastham, "Maglev: A Realistic Option for the Nineties." In *Magnetic Levitation Technology for Advanced Transit Systems,* A collection of papers presented at SAE Conference and Exposition on Future Transportation Technology, Society of Automotive Engineers, 1989.

[3] The Maglev Technology Advisory Committee, "Benefits of Magnetically Levitated High-Speed Transportation for the United States." Volume 1, Executive Report for the United States Senate Committee on Environment and Public Works. Published by Grumman Corp., Bethpage, NY, June 1989.

[4] R. Thornton, *Electronic Circuits.* MIT course notes, 1991.

[5] R. Thornton, "Why U.S. Needs a Maglev System." *Technology Review*, April 1991.

[6] F. Zhao, "Extracting and Representing Qualitative Behaviors of Complex Systems in Phase Spaces." *Proc. of the 12th International Joint Conference on Artificial Intelligence*, Morgan Kaufmann, 1991.

[7] F. Zhao, "Phase Space Navigator: Towards Automating Control Synthesis in Phase Spaces for Nonlinear Control Systems", *Proc. of the 3rd IFAC International Workshop on Artificial Intelligence in Real Time Control*, Pergaman Press, 1991.

Appendix A

The equilibria for $V_i = 140$ and $V_i = 300$:

```
; Vi = 140
((#(140. 0. 200.)              ; equilibrium point #(x y z)
  (-17.004+22.963i             ; eigenvalue 1
   -17.004-22.963i             ; eigenvalue 2
   24.007)                     ; eigenvalue 3
  (#(.23604 .97174 0)          ; eigenvector 1
   #(.51331 -.55588 .65384)    ; eigenvector 2
   #(.30157 .73255 .61027))    ; eigenvector 3
  saddle))                     ; stability type

; Vi = 300
((#(300. 0. 428.57)            ; equilibrium point #(x y z)
  (-21.411+21.394i             ; eigenvalue 1
   -21.411-21.394i             ; eigenvalue 2
   21.394)                     ; eigenvalue 3
  (#(.54819 .83636 0)          ; eigenvector 1
   #(.43085 -.65947 .616)      ; eigenvector 2
   #(.23229 .71052 .66423))    ; eigenvector 3
  saddle))                     ; stabi'ity type
```

Appendix B

This appendix contains the initial, switching, and final points of the synthesized reference trajectories starting from four different initial states, as shown in Figure 6 and 7. Each point in the print-out is a vector of (t, x, y, z).

```
; trajectory 1
(init-pt #(0. 140. 0. 220.))
(switch-pt #(.013441 162.98 4.4416 221.42))
(last-pt #(.12704 139.39 .078872 201.75))

; trajectory 2
(init-pt #(0. 140. 0. 280.))
(switch-pt #(.10156 276. -74.214 338.79))
(last-pt #(.32041 139.26 -.19212 196.51))

; trajectory 3
(init-pt #(0. 140. 0. 290.))
(switch-pt #(.19536 264.69 -105.03 340.68))
(last-pt #(.42865 142.4 3.2661 202.69))

; trajectory 4
(init-pt #(0. 140. 0. 300.))
(init #(0. 140. 0. 300.) is outside controllable region)
```